Study of cytokine induced neuropathology by high resolution proton NMR spectroscopy of rat urine

Julian L. Griffin[a,*], Daniel C. Anthony[b], Sandra J. Campbell[b], Jack Gauldie[c], Fernando Pitossi[d], Peter Styles[e], Nicola R. Sibson[e]

[a]*Department of Biochemistry, University of Cambridge, Tennis Court Road, Cambridge CB2 1QW, UK*
[b]*Molecular Neuropathology Laboratory, University of Southampton, Southampton, UK*
[c]*Department of Pathology and Molecular Medicine and Centre for Gene Therapeutics, McMaster University, Hamilton, Ont., Canada*
[d]*Foundation Leloir Institute, Buenos Aires, Argentina*
[e]*Department of Biochemistry, University of Oxford, Oxford, UK*

Received 13 February 2004; revised 15 April 2004; accepted 16 April 2004

Available online 24 May 2004

Edited by Thomas L. James

Abstract Multiple sclerosis is a major cause of non-traumatic neurological disability. The identification of markers that differentiate disease progression is critical to effective therapy. A combination of NMR spectroscopic metabolic profiling of urine and statistical pattern recognition was used to detect focal inflammatory central nervous system (CNS) lesions induced by microinjection of a replication-deficient recombinant adenovirus expressing TNF-α or IL1-β cDNA into the brains of Wistar rats. These animals were compared with a group of naïve rats and a group of animals injected with an equivalent null adenovirus. Urine samples were collected 7 days after adenovirus injection, when the inflammatory lesion is maximally active. Principal components analysis and Partial Least Squares-Discriminate analysis of the urine ^{1}H NMR spectra revealed significant differences between each of the cytokine adenovirus groups and the control groups; for the TNF-α group the main differences lay in citrate and succinate, while for the IL-1β group the predominant changes occurred in leucine, isoleucine, valine and myo-inositol. Thus, we can identify urinary metabolic vectors that not only separate rats with inflammatory lesions in the brain from control animals, but also distinguish between different types of CNS inflammatory lesions.

Keywords: Multiple sclerosis; Metabolomics; Metabonomics; Pattern recognition

1. Introduction

Multiple sclerosis (MS) is an immune-mediated disease of the central nervous system (CNS), characterised by demyelination, axonal loss, T cell and macrophage recruitment, and blood–brain barrier breakdown [1]. Lesions are often clinically silent and only detectable by cranial MRI. Anti-inflammatories have been shown to reduce periods of relapse and lesion spread during relapsing-remitting MS, while steroids are believed to slow the onset of secondary-progressive MS [2]. However, a continuous suppression of the immune system is undesirable. Consequently, it is of importance to identify easily accessible biological markers that enable reliable differentiation of the different phases of the disease.

Monitoring disease progression using body fluids has been applied previously to both MS patients and animal models [3,4], but these studies examined predetermined metabolites and had mixed success. High resolution ^{1}H NMR spectroscopic analysis of biofluids, and in particular urine and blood plasma, has become increasingly more common in the pharmaceutical industry's drug safety assessment process as a method for identifying target organ toxicity through urinary biomarkers [5,6]. Such metabonomic/metabolomic analysis has also recently been extended to predicting the presence and severity of coronary artery disease in humans [7]. This approach of biofluid metabolic profiling and statistical pattern recognition requires no a priori knowledge, identifying metabolites solely according to their correlated variation between treatment groups [8]. Furthermore, multivariate pattern recognition techniques such as principal components analysis (PCA) can identify distinct patterns of metabolites whose variation as a whole is characteristic of the disease, rather than rely on the identification of a unique biomarker of the disease [8].

Using such an approach 't Hart et al. [9] identified characteristic biochemical patterns in the urines of MS patients and in marmosets following experimental autoimmune encephalopathy (EAE). This study found that there were a number of changes in the composition of organic chemicals in the urine of marmosets following EAE, with the region between 0.5 and 3.5 ppm being important in distinguishing this group from controls. However, there are a number of metabolites found in this spectral region, and thus, the model did not provide an insight into the mechanisms being monitored. Furthermore, the EAE model produces large lesions, unlike the more focal lesions usually found in MS. However, their approach was also able to build a pattern recognition model that was 65% accurate in distinguishing urine from MS patients compared with healthy individuals and patients suffering from other neurological disorders, suggesting that biofluid NMR could be used to monitor MS.

The principal mediators of inflammatory responses in the body are the cytokines, a family of small, soluble proteins which modulate the immune system. Two key proinflammatory cytokines are interleukin-1β (IL-1β) and tumour necrosis

* Corresponding author. Fax: 44-0-1223-760002.
E-mail address: jlg40@mole.bio.cam.ac.uk (J.L. Griffin).

0014-5793/$22.00
doi:10.1016/j.febslet.2004.04.096

factor-α (TNF-α). Expression of IL-1β and TNF-α has been found to be associated with a broad spectrum of CNS injury and disease, including MS [10,11]. The aim of this study was to determine whether a combination of NMR spectroscopic metabolic profiling of urine samples and statistical pattern recognition could detect the presence of IL-1β and TNF-α induced CNS lesions and distinguish between the distinct neuropathologies caused. We have identified urinary metabolic perturbations that separate rats with inflammatory CNS lesions from control animals and which distinguish between two different types of inflammatory lesion in the brain. These findings suggest that this approach may be useful for following the progression and treatment of MS in humans in the early stages of the disease by monitoring the metabolic signatures associated with a particular cytokine response.

2. Materials and methods

2.1. Animal procedures

A focal inflammatory lesion in the left striatum of adult male Wistar rats was induced by microinjection of a replication-deficient recombinant adenoviral vector [12,13]: (i) adenovirus expressing murine membrane-bound TNF-α cDNA (Ad5TNF-α_m) ($n = 7$); (ii) adenovirus expressing murine IL-1β cDNA (Ad5IL-1β) ($n = 7$); and (iii) an adenovirus with no insert in the E1 region (AdDL70) (a control group where no cytokine is induced; $n = 5$). Animals were anaesthetised with 2.5% isoflurane in 70% N_2O:30% O_2 and injected stereotaxically over a 10-minute period (Bregma +1 mm, 3 mm lateral, depth 4 mm) with 10^7 PFU of adenovirus in 1 μl of saline using a <50 μm-tipped glass pipette. Urine samples were collected from animals 7 days after adenovirus injection, at which time previous immunocytochemical analysis demonstrated activation of resident microglia, and maximal leukocyte recruitment to the brain [12,13]. At seven days the histological features of the lesions induced by IL-1β and TNF-α are well characterised and distinct, but at earlier time points the lesions are less specific in terms of the leukocyte recruitment profile. Urine samples were also acquired from non-injected control animals ($n = 2$) for comparison. Urine samples were collected from each individual animal by gently depressing the abdomen of the animals to encourage them to urinate. This procedure avoided faecal contamination of the urine. Urine was frozen and stored at −80 °C until examined by NMR spectroscopy. All procedures were approved by the United Kingdom Home Office.

2.2. Histological analysis

Following urine collection, animals were deeply anaesthetised with sodium pentobarbitone and transcardially perfused with 200 ml of 0.9% heparinised saline followed by 200 ml periodate lysine paraformaldehyde. After dissection, the brains were post-fixed for several hours in the fixative and then immersed in 30% sucrose buffer for 24 h to cryoprotect. The tissue was then embedded in Tissue Tek (Miles Inc, Elkhart, USA) and frozen in isopentane at −40 °C. Cresyl violet-stained sections (50 μm) were examined for signs of neuronal damage and for the presence of leukocytes. Immunohistochemistry was used to confirm the presence and distribution of specific cell populations. Frozen, 10 μm thick, serial sections were cut from the fixed tissue and mounted on gelatin-coated glass slides. Antigens were detected using a three-step indirect method [14]. Polymorphonuclear neutrophils were identified using the anti-neutrophil serum HB199 [15] and macrophages were identified using the monoclonal antibodies ED1 [16], which stains most macrophage populations including recruited monocytes, but not quiescent microglia. T and B cells were identified using an in-house mouse monoclonal antibody, OX42 (available on request from D.C.A.). Neurones were identified using anti-NeuN monoclonal antibody (Chemicon International) and 25-μm-thick frozen sections were processed for cholinesterase histochemistry using acetylthiocholine as substrate.

2.3. NMR spectroscopy

Urine (300 μl) was diluted in a buffered phosphate solution (210 μl of 0.2 M Na_2HPO_4/ 0.04 M NaH_2PO_4, pH 7.4, 0.1% sodium azide) and 90 μL of TSP (3-trimethylsilyl-1-[2,2,3,3,-$^2H_4$] propionate; 1 mM final concentration; internal standard) both in deuterium oxide. NMR spectra of urine were acquired at 600 MHz ^{1}H NMR frequency using a standard solvent suppression pulse sequence (NOESYPR1D, mixing time = 50 ms, relaxation delay = 1.75 s) and a Bruker AVANCE spectrometer (Bruker Gmbh, Germany). Spectra were subdivided into 0.04 ppm integral regions and integrated, reducing each spectrum to 200 independent variables between 0.5–4.28 and 6.04–9.96 ppm and forming the matrix for pattern recognition [17]. The region between 4.28 and 6.04 ppm was excluded to avoid the region of water suppression and the broad resonance from urea, both of which represents highly variable regions in the spectra. PCA and Partial Least Squares-Discriminate analysis (PLS-DA) were applied within the software package SIMCA 9.0 (Umetrics, Umea, Sweden). Prior to pattern recognition, the spectra (observables) were scaled using a Pareto scaling, where each integral region was centred about the mean and divided by the square route of the standard deviation of the mean [18]. PLS-DA is a supervised regression extension of PCA, where the algorithm is instructed of class membership and maximises the separation in multivariate space according to these classes. To test this supervised pattern recognition, the class membership of each spectrum was predicted by omitting each spectrum in turn from a PLS-DA model of the other spectra and predicting its class membership.

To confirm the assignments made from the one-dimensional ^{1}H NMR spectra, a urine sample from each treatment group was also examined using a gradient Correlation Spectroscopy (COSY) pulse sequence with solvent suppression. The COSYs were acquired with a 1.5 s relaxation delay, a sweep width of 8503 Hz, 16 acquisitions and 256 increments in the F1 dimension.

3. Results

3.1. Inflammatory lesions

The adenovirus injections caused focal over-expression of either membrane-bound TNF-α or IL1-β leading to the development of a focal inflammatory lesion in the left striatum (Fig. 1) that persisted for the seven day period. Injection of Ad5TNF-α_m gave rise to marked macrophage and T-cell recruitment to the brain (Fig. 1(a)), followed by demyelination and neuronal loss without overt clinical signs. In contrast, injection of Ad5IL-1β gave rise to marked neutrophil recruitment to the brain (Fig. 1(b)), again followed by demyelination, but without any overt neuronal cell death. Injection of the null adenovirus (AdDL70) yielded no histopathological signs of inflammation or injury that were visible after 7 days (data not shown). TNF-α, IL-1β and IL-6 were not detected by ELISA in the serum of any animal, indicating that the expression of cytokines was restricted to the CNS and that they did not leak in any measurable amount into the circulation (data not shown). No weight changes were detected in any of the animals during the study.

3.2. Urine analysis

High resolution ^{1}H NMR spectroscopy produced spectra of the urine samples that readily identified and quantified over 30 metabolites. The urinary metabolites were identified by reference to previous literature values [19] and the use of COSY spectra (Fig. 2). However, while the spectra were superficially similar, the proportion of these metabolites appeared to be characteristic of the insult induced (Fig. 3). The urine from rats treated with Ad5TNF-α_m produced spectra that were dominated by citrate, 2-oxoglutarate and creatine compared with the control group. On the other hand, the urine of rats exposed to Ad5IL-1β had increased concentrations of leucine, isoleucine, valine, isobutyrate, *N*-acetyl glycoproteins and acetate compared with the other two groups. To place the visual

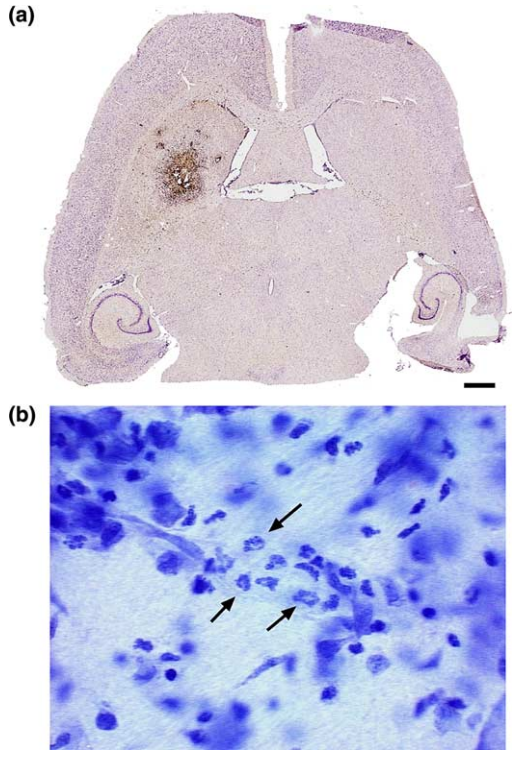

Fig. 1. (a) Immunolocalisation of activated microglia and recruited macrophages (brown stained OX42-positive cells) delineating the lesion on a horizontal section one week after an injection of 10^7 pfu replication-deficient recombinant adenovirus expressing murine TNF-α cDNA. (b) Immunolocalisation of recruited neutrophils (identified by the nuclear morphology) delineating the lesion on a coronal section one week after an injection of 10^7 pfu replication-deficient recombinant adenovirus expressing murine IL-1β cDNA. In both cases, cresyl violet was used to counter-stain the nuclei. Scale bar = 1 mm.

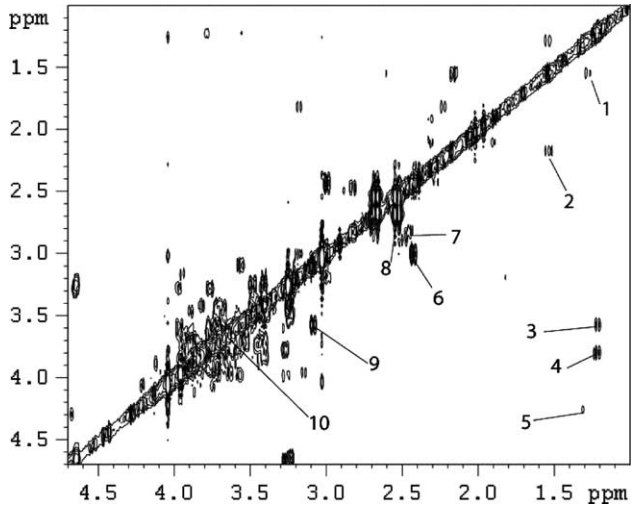

Fig. 2. 600.13 MHz COSY spectrum of rat urine from a rat exposed to Ad5IL-1β used to confirm assignments of coupled resonances. Key: 1, *n*-butyrate; 2, *n*-butyrate; 3, valine; 4, leucine; 5, lactate; 6, 2-oxoglutarate; 7, aspartate; 8, citrate; 9, lysine; 10, glucose containing region.

inspections in a statistical context, multivariate pattern recognition was applied.

Applying PCA to the data set of urine spectra, separation of the profiles from treated rats was across PC1 and PC2, with the two treated groups showing distinct perturbations from the combined control data set across either PC1 (Ad5IL-1β treated group) or PC2 (Ad5TNF-α_m treated group) (Fig. 4(a)). The combined PCs represented 58% of the variation in the data set. Examining the loadings that contributed to the separation of Ad5IL-1β treated rats from control animals, this was caused by increases in leucine, isoleucine, and valine (δ 0.96, 1.16, 1.12; where δ is the chemical shift of the centre of the 0.04 ppm region identified by the pattern recognition), isobutyrate (δ 1.12, 1.16), ethanol (1.16; a contaminant) and glucose (δ 3.44, 3.58, 3.88). This separation was still apparent when the resonance region corresponding to ethanol was removed from the model. Ad5TNF-α_m treated animals had increased excretion of citrate (δ 2.68, 2.54) and 2-oxoglutarate (δ 2.44, 3.00) (Fig. 4(b)). During this analysis the rats receiving no treatment (naives) and the sham controls (receiving a null adenovirus) mapped to the same PC location, and hence were treated as a single control group.

Repeating this analysis using PLS-DA, to produce orthogonal vectors that maximise the difference between groups, the separation between groups was also apparent. PLS-DA produced a four component model that separated all three groups across PLS-DA components 1 and 2 (Fig. 4(c)). For the Ad5IL-1β treated group, separation from the control group was caused by increases in leucine, isoleucine and valine (δ 0.96, 1.12), isobutyrate (δ 1.16) glucose (δ 3.44, 3.56, 3.88), creatine (δ 3.04, 3.96) and trimethylamine oxide (TMAO) (δ 3.24). Again Ad5TNF-α_m treated animals demonstrated increased excretion of citrate and 2-oxoglutarate (Fig. 4(d)).

As the separation in the PLS-DA model was caused by a number of high concentration metabolites which would have significant leverage over the model, to identify other potential biomarkers of effect, the above metabolites were excluded and a new PLS-DA model produced. Again the urine from animals exposed to Ad5IL-1β and Ad5TNF-α_m were separated from the combined control group. Animals exposed to Ad5IL-1β had increased concentrations of cysteine (δ 3.08, 3.12), taurine (δ 3.40) and acetate (δ 1.96), while animals exposed to Ad5TNF-α_m had increased concentrations of succinate (δ 2.40), hippurate (δ 7.84, 7.64, 7.52) and phenylacetylglycine (δ 7.36, 3.76, 3.68). Subsequent exclusion of these metabolites in addition to those mentioned above caused the PLS-DA model to fail in distinguishing the three groups.

Rebuilding PLS-DA models but sequentially excluding from the model training process one spectrum and subsequently predicting the class membership of the animal using the built model allowed us to estimate the predictive ability of our approach. Of a total of 19 animals, 15 were correctly classified into the right treatment group using this process. Thus, the model's predictive power of ~79% was far greater than that produced by chance (33%).

As the multivariate analysis demonstrated that the two exposure groups separated in opposite directions from the control group, the data were also processed as a two-way comparison (models not shown). The animals exposed to Ad5IL-1β had an increased concentration of taurine (δ 3.28, 3.40) and decreased concentrations of hippurate (δ 7.84, 7.52), succinate (δ 2.40) and citrate (δ 2.72) compared with the combined control group. The animals exposed to Ad5TNF-α_m had increased concentrations of glucose (δ 3.72, 3.64, 3.60) and phenylacetylglycine (δ 7.36, 3.76, 3.68). Finally, the two exposure groups could be separated with animals exposed to

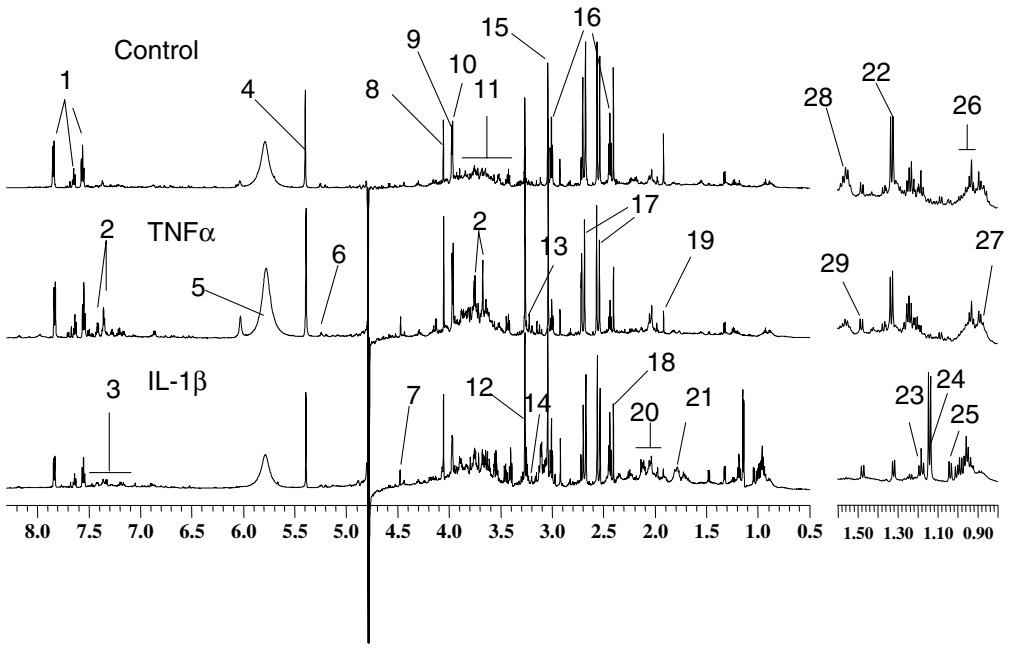

Fig. 3. 600.13 MHz spectra of rat urine from either a control animal or animals exposed to focal lesions from Ad5IL-1β or Ad5TNF-α_m . Spectra were acquired using the NOESYPR1D pulse sequence for solvent suppression. Key: 1, hippurate; 2, phenylacetylglycine (with traces of phenylalanine in aromatic region); 3, tyrosine; 4 allantoin; 5, urea; 6, α-glucose; 7, *N*-methylnicotinamide; 8, creatinine; 9, hippurate; 10, creatine 11, glucose and amino acid CH protons; 12, TMAO; 13, phosphocholine; 14, choline; 15, creatine and creatinine; 16, 2-oxoglutarate; 17, citrate; 18, succinate; 19, acetate; 20, *N*-acetyl glycoproteins; 21, tentatively assigned to bile acids; 22, lactate; 23, ethanol (contaminant); 24, isobutyrate; 25, valine; 26, leucine, isoleucine and valine; 27, *n*-butyrate; 28, *n*-butyrate; 29, alanine.

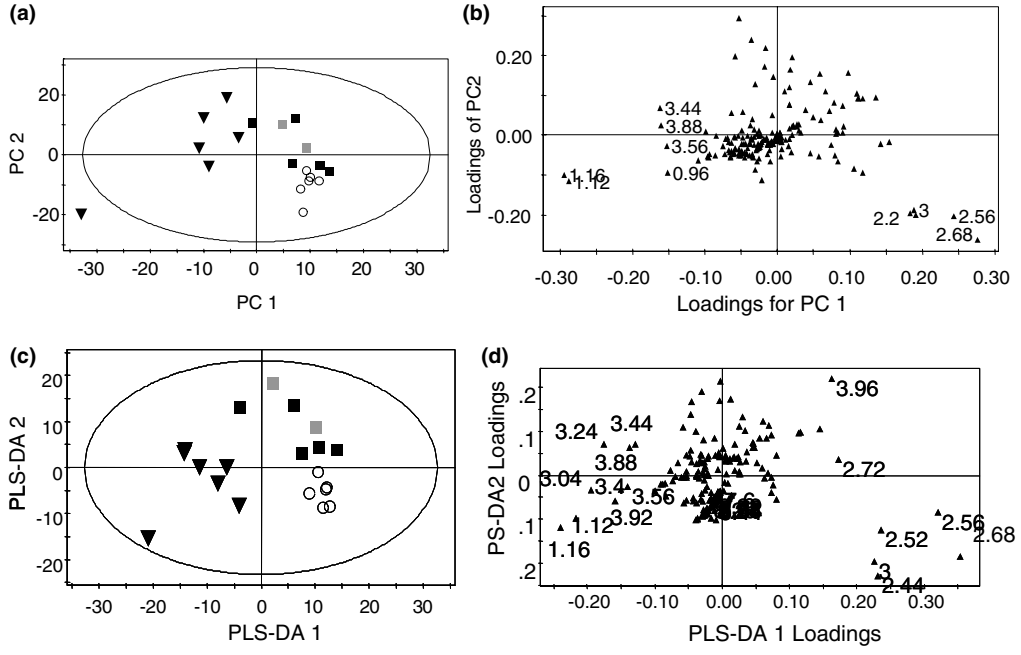

Fig. 4. Pattern recognition of the urinary profiles separated animals exposed to focal lesions from Ad5IL-1β or Ad5TNF-α_m compared with a control group consisting of control animals which either received no injection ($n = 2$) or an injection of a control adenovirus with no insert in the E1 region. (a) PCA scores scatter plot for the first two PC components formed by analysis of the variation in the urinary spectral profiles. (b) The corresponding Loadings plot highlighting which spectral regions were important in this classification (metabolites in a similar vectoral direction in the loadings plot as the spectral profiles in the scores scatter plot are most discriminating for the clusterings detected). (c) The supervised technique PLS-DA analysis of the data produced a better separation. (d) The loadings plot for the PLS-DA model, showing which metabolite regions were important for this classification. Key: ■, spectra of urine from control group (null adenovirus); ■, spectra from untreated animals; ▼, spectra of urine from rats exposed to Ad5IL-1β; ◯, spectra from rats exposed to Ad5TNF-α_m.

Ad5IL-1β having an increased concentration of taurine (δ 3.28, 3.40) and decreased concentrations of citrate (δ 2.72), succinate (δ 2.40) and hippurate (δ 7.84, 7.52) compared with animals exposed to Ad5TNF-α_m.

4. Discussion

In this study, we have identified urinary metabolic vectors that separate rats with inflammatory CNS lesions from control animals. Furthermore, these vectors distinguish between two different types of inflammatory lesion in the brain. These findings suggest that the combination of NMR spectroscopic urinary profiling and statistical pattern recognition may be a useful approach for following disease progression and treatment in individuals with inflammatory lesions in the brain, such as MS patients.

MS is associated with chronic expression of the key proinflammatory cytokines, TNF-α and IL1-β [20]. In this study, we have used an adenoviral vector to induce chronic endogenous expression of either IL-1β or TNF-α in the rat brain. We have previously demonstrated that, in contrast to their effects in the periphery, these cytokines give rise to markedly different inflammatory profiles within the CNS following single bolus microinjection into the brain parenchyma [13,21–23]. Similarly, in the current study expression of IL-1β led to predominantly polymorphonuclear leukocyte-mediated inflammatory response, whilst TNF-α gave rise to a predominantly monocyte-mediated lesion. Significant differences were found between these groups in terms of their urinary analysis, suggesting that the different types of inflammatory lesions have distinctly different consequences in the periphery.

Specifically, the Ad5IL-1β treated group predominantly exhibited increases in leucine, isoleucine, valine, *n*-butyrate and glucose, whilst the Ad5TNF-α_m treated animals demonstrated increased excretion of citrate, 2-oxoglutarate and succinate. Given the focal nature of the lesions induced in this study, metabolite changes detected in urine are likely to be a secondary effect of the lesion. Indeed, it is known that following infection or injury to the CNS, the liver releases acute phase proteins [24]. A significant component of the hepatic acute phase response is the release of chemokines by the liver, which control and amplify the CNS response to injury by controlling the rate, timing, magnitude and composition of leukocyte recruitment to the damaged brain and to the liver. We have found that enzyme markers of liver tissue injury are increased in the serum following generation of a focal inflammatory lesion in the brain [24–26]. Thus, the different urinary biomarkers may reflect the different responses in the liver to Ad5IL-1β and Ad5TNF-α_m.

However, increased excretion of the organic acids citrate, succinate and 2-oxoglutarate are commonly seen in drug toxicity studies in rats [25–28]. This suggests that the major biomarkers associated with exposure to Ad5TNF-α_m reflect a general metabolic perturbation related to stress. However, if similar metabolic responses are detectable in MS patients, these general metabolic markers of stress could still be used as surrogate markers for relapse. Furthermore, these metabolites represent those most responsible for the classification and will not represent all the metabolites perturbed in the urine sample. We were able to identify and quantify ~30 metabolites in this study, but this excluded many smaller resonances. These may either provide unique biomarkers for Ad5TNF-α_m and Ad5IL-1β lesions, or alternatively, the proportion of metabolites could be used to reconstruct metabolic correlation maps, akin to those constructed for yeast and plants [29], which might suggest which pathways are perturbed.

While the intermediate steps to the urine profiles are unclear, it remains the case that we were able to distinguish between distinct pathologies with the brain and raises the possibility that the pathogenesis of inflammatory lesions and total lesion load might be followed by applying metabolomics/metabonomics to urine analysis. These experiments were performed on a laboratory strain of rat, fed on a controlled diet, and applying such an approach directly to humans will be confounded by greater physiological and dietary variation. However, urine samples can be monitored across time on an individual basis, to identify when that individual enters a relapse. Indeed, such temporal studies are particularly amenable to batch processing pattern recognition techniques that use a time component to identify outliers [30] (i.e., the relapse episode). Furthermore, systemic biomarkers may also be apparent in blood plasma, with as little as 2-5 μl of plasma being required for such analysis [31]. Indeed, metabolic profiling has already been demonstrated to be effective at distinguishing severity in coronary artery disease [7] and high blood pressure [32] through biomarkers detected in blood plasma. However, urine has a number of distinct advantages over examining blood plasma directly. Blood plasma contains lipoproteins and lipids which can obscure a significant amount of the spectral sweep width. It is relatively closely controlled in terms of composition, and would be expected to be perturbed less than urine, where metabolites can be concentrated significantly. Also the metabolic profiles of blood plasma provide a snapshot of metabolism, rather than an average of the metabolic changes over a period of time. Thus, if we had used blood plasma we might have missed key metabolic changes. In conclusion, this study demonstrates that the use of metabolic profiling by NMR spectroscopy for the treatment of MS is now a realistic possibility.

Acknowledgements: This work was supported by the Royal Society, UK (J.L.G.) and the Medical Research Council, UK (N.R.S., P.S.).

References

[1] Trapp, B.D., Bo, L., Mork, S. and Chang, A. (1999) J. Neuroimmunol. 98, 49–56.
[2] Rieckmann, P. and Smith, K.J. (2001) Trends Neurosci. 24, 435–437.
[3] Mehta, P.D., Cook, S.D., Coyle, P.K., Troiano, R.A., Constantinescu, C.S. and Rostami, A.M. (1998) Mult. Scler. 4, 254–256.
[4] Sorensen, P.S. (1999) Mult. Scler. 5, 287–290.
[5] Lindon, J.C., Nicholson, J.K., Holmes, E., Antii, H., Bollard, M.E., Keun, H., Beckonert, O., Ebbels, T.M., Reily, M.D. and Robertson, D., et al. (2003) Toxicol. Appl. Pharmacol. 187, 137–146.
[6] Nicholson, J.K., Connelly, J., Lindon, J.C. and Holmes, E. (2003) Nat. Rev. Drug Discov. 1, 153–161.
[7] Brindle, J.T., Antti, H., Holmes, E., Tranter, G., Nicholson, J.K., Bethell, H.W.L., Clarke, S., Schofield, P.M., McKilligin, E., Mosedale, D.E. and Grainger, D.J. (2002) Nat. Med. 8, 1439–1444.
[8] Lindon, J.C., Holmes, E. and Nicholson, J.K. (2001) Prog. Nucl. Magn. Reson. 39, 1–40.
[9] 't Hart, B.A., Vogels, J.T.W.E., Spijksma, G., Brok, H.P.M., Polman, C. and van der Greef, J. (2003) J. Neurol. Sci. 212, 21–30.
[10] Olsson, T. (1995) Neurology 45, S11–S15.

[11] Ledeen, R.W. and Chakraborty, G. (1998) Neurochem. Res. 23 (3), 277–289.
[12] Kolb, M., Margetts, P.J., Anthony, D.C., Pitossi, F. and Gauldie, J. (2001) J. Clin. Invest. 107, 1529–1536.
[13] Sibson, N., Blamire, A., Gauldie, J., Perry, V., Styles, P. and Anthony, D. (2002) Brain 125, 2446–2459.
[14] Hsu, S.M., Raine, L. and Fanger, H. (1981) Am. J. Clin. Pathol. 75, 816–821.
[15] Anthony, D.C. et al. (1998) J. Neuroimmunol. 87, 62–72.
[16] Dijkstra, C.D., Dopp, E.A., Joling, P. and Kraal, G. (1985) Immunology 54, 589–599.
[17] Beckwith-Hall, B.M., Nicholson, J.K., Nicholls, A.W., Foxall, P.J., Lindon, J., Connor, S.C., Abdi, M., Connelly, J. and Holmes, E. (1998) Chem. Res. Toxicol. 11, 260–272.
[18] Eriksson, L, Johansson, E., Kettaneh-Wold, N. and Wold, S. (1999) Introduction to Multi- and Megavariate Data Analysis using Projection Methods, Umetrics, Umea, Sweden.
[19] Fan, T.W. (1996) Prog. Nucl. Magn. Reson. Spectrosc. 28, 161–219.
[20] Sharief, M.K. and Hentges, R. (1991) N. Engl. J. Med. 325, 467–472.
[21] Anthony, D.C., Bolton, S.J., Fearn, S. and Perry, V.H. (1997) Brain 120, 435–444.
[22] Blamire, A.M., Anthony, D.C., Rajagopalan, B., Sibson, N.R., Perry, V.H. and Styles, P. (2000) J. Neurosci. 20, 8153–8159.
[23] Schnell, L., Fearn, S., Schwab, M.E., Perry, V.H. and Anthony, D.C. (1999) J. Neuropathol. Exp. Neurol. 58, 245–254.
[24] Campbell, S.J., Hughes, P.M., Iredale, J.P., Wilcockson, D.C., Waters, S., Docagne, F., Perry, V.H. and Anthony, D.C. (2003) FASEB J. 17, 1168–1170.
[25] Wilcockson, D.C., Campbell, S.J., Anthony, D.C. and Perry, V.H. (2002) J. Cereb. Blood Flow Metab. 22 (3), 318–326.
[26] Holmes, E., Nicholls, A.W., Lindon, J.C., Ramos, S., Spraul, M., Neidig, P., Connor, S.C., Connelly, J,, Damment, S.J., Haselden, J. and Nicholson, J.K. (1998) Chemometr. Intell. Lab. Syst. 44, 245–255.
[27] Waters, N.J., Holmes, E., Williams, A., Waterfield, C.J., Farrant, R.D. and Nicholson, J.K. (2001) Chem. Res. Toxicol. 14 (10), 1401–1412.
[28] Griffin, J.L., Walker, L.A., Shore, R.F. and Nicholson, J.K. (2001) Chem. Res. Toxicol. 14 (10), 1428–1434.
[29] Fiehn, O. (2001) Comp. Funct. Genom. 2, 155–168.
[30] Azmi, J., Griffin, J.L., Antti, H., Shore, R.F., Johansson, E., Nicholson, J.K. and Holmes, E. (2002) Analyst 127 (2), 271–276.
[31] Griffin, J.L., Nicholls, A.W., Keun, H.C., Mortishire-Smith, R.J., Nicholson, J.K. and Kuehn, T. (2002) Analyst 127 (5), 582–584.
[32] Brindle, J.T., Antti, H., Holmes, E., Tranter, G., Nicholson, J.K., Bethell, H.W.L., Clarke, S., Schofield, P.M., McKilligin, E., Mosedale, D.E. and Grainger, D.J. (2003) Analyst 128, 32–36.